

Indirect X-Ray Line Formation Processes in Highly Charged Barium

P. Beiersdorfer, A. L. Osterheld, M. H. Chen, J. R. Henderson, D. A. Knapp, M. A. Levine, R. E. Marrs, K. J. Reed, M. B. Schneider, and D. A. Vogel

High Temperature Physics Division, University of California, Lawrence Livermore National Laboratory, Livermore, California 94550

(Received 9 November 1989)

We have studied indirect excitation processes contributing to the x-ray line emission of neonlike barium (Ba^{46+}) interacting with an electron beam. Techniques are presented which resolve the contributions due to electron capture by fluorinelike ions and inner-shell ionization of sodiumlike ions from contributions due to direct electron-impact excitation and radiative cascades. The strength of resonance excitation of the $2p$ - $3s$ magnetic quadrupole line through intermediate levels $4lnl'$ ($n=5,6$) is measured to equal $S=(2.8 \pm 0.8) \times 10^{-19} \text{ cm}^2 \text{ eV}$.

PACS numbers: 34.80.Kw, 32.30.Rj

Atomic line radiation can be excited by many mechanisms. In a plasma with a Maxwellian electron distribution virtually all excitation processes can occur simultaneously. This is not the case for ions interacting with a monoenergetic electron beam. Electron beams can be used to select and study atomic excitation processes isolated from each other. Such studies are of importance for proper modeling of the line emission observed from internal-confinement fusion,¹ magnetic fusion,² and astrophysical sources.³

In the following we report a systematic investigation of x-ray line formation due to indirect excitation mechanisms in a highly charged ion interacting with an electron beam. For the measurement we use the Livermore electron-beam ion trap (EBIT). The device employs a 100–300-mA electron beam to generate, confine, and excite high- Z ions.^{4,5} A particular charge distribution is selected by appropriate choices of the beam energy. Unlike facilities EBIS or ECR,⁶ which are ion sources, EBIT is specifically designed as an x-ray source, and the interaction of the electron beam with trapped ions is studied by observing the x-ray emission.

Our investigation focuses on the magnetic quadrupole transition $(2p_{3/2}^5 3s_{1/2})_{J=2} \rightarrow 2p^6 \ ^1S_0$ in neonlike barium (Ba^{46+}). The transition, labeled $M2$, was chosen because it can be excited by other than direct electron collisions and radiative cascades from higher-lying levels: It also is susceptible to indirect excitation processes involving ions of neighboring charge states. Its upper level is the lowest-lying excited level in a neonlike ion, and, because of its high total angular momentum, is the terminal level for many yrast transitions, i.e., transitions between levels of maximum angular momentum. The line was first observed and identified in solar spectra of neonlike iron⁷ and in laboratory spectra of the transition elements chromium, iron, and nickel on the Tokamak Fontenay-aux-Roses.⁸

Processes that can lead to the excitation of line $M2$ are direct electron-impact excitation,

$$2p^6 + e^- \rightarrow 2p_{3/2}^5 3s_{1/2} + e^-, \quad (1)$$

radiative cascades following excitation,

$$2p^6 + e^- \rightarrow 2p_{3/2}^5 nl + e^- \rightarrow 2p_{3/2}^5 3s_{1/2} + e^- + h\nu, \quad (2)$$

radiative electron capture by fluorinelike barium,

$$2p_{3/2}^5 + e^- \rightarrow 2p_{3/2}^5 3s_{1/2} + h\nu, \quad (3)$$

inner-shell ionization of sodiumlike barium,

$$2p^6 3s + e^- \rightarrow 2p_{3/2}^5 3s_{1/2} + 2e^-, \quad (4)$$

$$2s^2 2p^6 3s + e^- \rightarrow 2s_{1/2} 2p^6 3s_{1/2} + 2e^-$$

$$\rightarrow 2s^2 p_{3/2}^5 3s_{1/2} + 2e^-,$$

and resonance excitation,

$$2p^6 + e^- \rightarrow 2p_{3/2}^5 nln'l' \rightarrow 2p_{3/2}^5 3s_{1/2} + e^-. \quad (5)$$

By contrast, the neonlike electric dipole transition $(2p_{3/2}^5 3d_{5/2})_{J=1} \rightarrow 2p^6 \ ^1S_0$, which we label $3D$, is almost exclusively populated by direct electron-impact collisions, Eq. (1). Cascades from levels $n \geq 3$ are predicted to contribute less than a few percent of the total excitation flux. The same is true for electron capture, Eq. (3). Inner-shell ionization cannot contribute to its excitation, as the electron density in EBIT is low enough ($\leq 6 \times 10^{12} \text{ cm}^{-3}$) to ensure single-collision conditions and the absence of metastables. Because of this insensitivity to excitation processes other than direct electron collisions the intensity of line $3D$ provides a good reference for determining the intensities of other neonlike transitions. We use this in the following to measure the intensity of $M2$ relative to $3D$. We note that the excitation cross section of $3D$ was measured recently by Marrs *et al.*⁴ Using their values, the cross section of a given line can be inferred from a relative measurement involving the $3d \rightarrow 2p$ transition.

The neonlike line intensities are measured as a function of electron-beam energy using a flat-crystal spectrometer in a plane perpendicular to the beam direction. The spectrometer employs a silicon (220) crystal and a position-sensitive proportional counter. The Bragg angle is near 45° so that mostly radiation with electric-field

vector parallel to the beam is diffracted; x rays with electric-field vectors perpendicular to the beam are almost completely absorbed by the crystal and are not counted. Barium is given off by the cathode of the electron gun and continuously enters the trap so that its spectrum is observed in quasi-steady-state. On average, one spectrum is obtained in 90 min.

The measured ratio $M2/3D$ versus electron energy is plotted in Fig. 1. The figure also shows predictions from a collisional-radiative model that includes the ground state and the 156 excited levels in the configurations $2s2p^6nl$ and $2s^22p^5nl$ with $n=3,4,5$. The model takes into account all $E1$ and $E2$, as well as relevant $M1$ and $M2$ radiative transitions, and all electron-impact collisions connecting these levels. Energy levels and radiative rates are computed in the relativistic, multiconfigurational parametric potential method.⁹ Electron-collision cross sections are obtained from quasirelativistic distorted-wave calculations.¹⁰

The theoretical intensity ratios have been normalized to measured values near 5.7 keV, where impact excitation of $n=3$ levels is the only direct contributor to the line emission. This is necessary because the calculations are for total cross sections and do not take into account that the line emission from EBIT is generally polarized.¹¹ We have made separate calculations for $3D$ of electron-impact excitation to magnetic sublevels using the method of Zhang, Sampson, and Clark.¹² These cal-

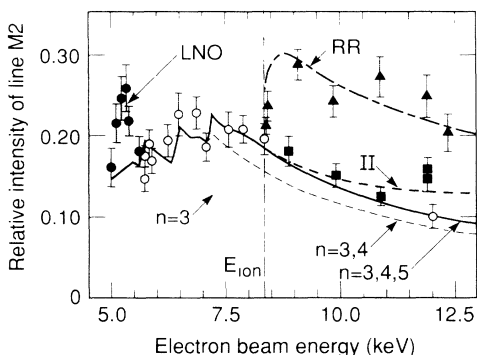


FIG. 1. Dependence of the relative intensity of line $M2$ on beam energy. The data are normalized to the intensity of line $3D$. Open circles reflect data excited predominantly by electron collisions and cascade feeding. Resonance excitation is strongest for data plotted as solid circles. Recombination of Ba^{47+} strongly affects data plotted as solid triangles; inner-shell ionization of Ba^{45+} affects the data plotted as solid squares. Also shown are the predictions from a collisional-radiative model which includes all $n=3$ levels (dotted line), all $n=3,4$ levels (dashed line), and all $n=3,4,5$ levels (solid line). The dot-dashed and long-short-dashed lines represent model calculations of the effects of inner-shell ionization (II) of Ba^{45+} and of radiative recombination (RR) of Ba^{47+} , respectively. In the latter calculation the radiative recombination coefficient has been increased by a factor of 5 to fit the data. E_{ion} denotes the ionization potential of Ba^{46+} at 8.33 keV.

culations predict a nearly constant polarization of $P=+0.40$ at 5.7 keV and $P=+0.44$ at 12.0 keV and thus justify a one-point normalization. The factor needed to match calculated with observed line ratios implies a polarization of $P=-0.05 \pm 0.10$ for $M2$.

Cascade feeding is an important excitation mechanism; as a result, agreement between data and theory is sensitive to the number of levels included in the model. Calculations that include only the $n=3$ excited states (37 levels including the ground state) and only the $n=3,4$ excited states (89 levels) are shown in Fig. 1 as dotted and dashed lines. The curves fit the data less well than the curve resulting from the 157-level model calculations. Inclusion of additional excited levels in the model may increase the computed intensities close to the ionization potential of Ba^{46+} , $E_{ion}=8.33$ keV. However, construction of such very large collisional-radiative models is not warranted until polarization effects are addressed in the calculations.

Resonance excitations¹³⁻¹⁶ involving intermediate configurations of the type $2p^54nl'$, $n \geq 4$ are seen to enhance the line intensities below $E \lesssim 5.7$ keV. Resonances involving $2s$ core electrons occur in the range $5.8 \lesssim E \lesssim 6.2$ keV, but do not seem to affect the line strongly.

The effect of electron capture on the intensity of $M2$ is demonstrated by the data in Fig. 1 for beam energies above the ionization potential E_{ion} of neonlike barium. The first set (solid triangles) is obtained in the presence of a considerable fraction of barium ions in the fluorine-like charge state so that recombination is an integral part of the processes occurring in the trap. We also measure the line intensities above E_{ion} without the effects of recombination. An ionization balance free of Ba^{47+} is established by setting the beam energy to 5.65 keV. The energy is then briefly ($\Delta t \approx 5$ msec) switched to a value above E_{ion} , where measurements are taken without significantly perturbing the ionization balance. The resulting line intensities at 9, 10, 11, and 12 keV are shown in Fig. 1 as solid squares.

A clear enhancement of the excitation cross section of $M2$ is found in the presence of fluorinelike ions. To estimate the effect of recombination, we have expanded our model to include radiative capture of beam electrons into levels $2s^22p^5nl$ ($n \leq 4$) followed by cascades. The modeling results are shown as the long-short-dashed line in Fig. 1. The target-ion density ratio Ba^{47+}/Ba^{46+} required for the calculations is determined experimentally from the ratios of fluorinelike and neonlike $3 \rightarrow 2$ transitions. We find that radiative recombination alone cannot account for the large increase in the line emission. To obtain the fit shown, it is necessary to increase recombination rates by a factor of 5. This implies that recombination processes other than radiative capture of beam electrons shape the ion kinetics in EBIT. Assuming charge exchange with nitrogen is the dominant recombination mechanism, we estimate a pressure of n_{N_2}

$\approx 10^{-9}$ – 10^{-8} Torr in the trap.¹⁷ This value is consistent with our usage of a nitrogen-gas jet to cool the ions,¹⁸ and is substantially higher than the density ($\leq 10^{-12}$ Torr) expected in a cryogenically pumped trap at liquid-helium temperature.

A second indirect excitation mechanism involves the inner-shell ionization of sodiumlike ions, which occurs for energies above 8.2 keV. Because the density ratio $\text{Ba}^{45+}/\text{Ba}^{46+}$, as determined experimentally from the ratios of sodiumlike and neonlike $3 \rightarrow 2$ transitions, is small in measurements with $E > E_{\text{ion}}$, the enhancement of the neonlike lines is expected to be small and cannot be conclusively inferred from the data in Fig. 1. Theoretical results assuming a ratio $\text{Ba}^{45+}/\text{Ba}^{46+} = 0.25$ are shown in Fig. 1 as the dot-dashed line.

We can identify the effect of inner-shell ionization by increasing the relative amount of sodiumlike ions. The results are shown in Fig. 2. In the figure we also plot the relative intensity of the electric quadrupole transition $2p_{3/2}^5 3p_{1/2} \rightarrow 2p_{6/1}^6 S_0$, labeled $E2L$, which cannot be excited via inner-shell ionization. Measurements are made by establishing a large relative abundance of Ba^{45+} at an energy near 5 keV (i.e., the LNO resonance) and briefly switching to 12 keV. Extrapolation to zero abundance of Ba^{45+} provides the line intensity in the absence of inner-shell ionization. These values are plotted as open circles in Fig. 2. As expected, inner-shell ionization enhances the $M2$ line, but does not affect the electric quadrupole line.

Our measurements allow us to determine the strength S of the LNO and LNP dielectronic resonances contributing to the excitation of $M2$ in the energy range 5.0–5.7 keV. S is defined as

$$S_{M2} \equiv \int_{LNO, LNP} \sigma(\text{g.s.}, M2, E) dE, \quad (6)$$

where $\sigma(\text{g.s.}, M2, E)$ is the cross section for resonance

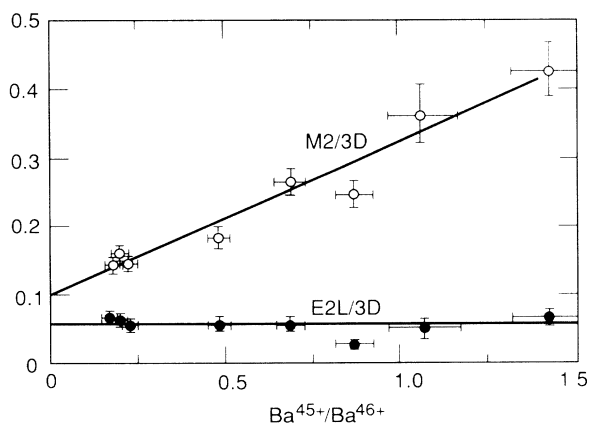


FIG. 2. Dependence of the intensities of lines $M2$ and $E2L$ on the relative abundance of sodiumlike and neonlike ions. The beam energy is 12 keV. The increase in intensity of line $M2$ is due to inner-shell ionization of sodiumlike ions.

excitation from the neonlike ground state to the excited level $M2$. Using the method of Chen and Reed¹⁵ and including cascade contributions from higher-lying neonlike levels, we calculate $S_{M2} = 3.5 \times 10^{-19} \text{ cm}^2 \text{ eV}$ and $S_{3D} = 1.0 \times 10^{-19} \text{ cm}^2 \text{ eV}$. For comparison, the calculated cross sections for electron-impact excitation of $M2$ and $3D$ at $E = 5.3$ keV (again including cascade contributions) are $\sigma_{\text{ex}}^{M2} = 9.8 \times 10^{-22} \text{ cm}^2$ and $\sigma_{\text{ex}}^{3D} = 3.5 \times 10^{-21} \text{ cm}^2$, respectively. Resonance excitation, therefore, enhances the emission of $M2$ by more than 50% in the energy range 5.0–5.7 keV, and that of $3D$ by less than 4%. Consequently, we can determine S_{M2} from the shaded area in Fig. 1 and by normalizing to σ_{ex}^{M2} ; we find $S = (2.8 \pm 0.8) \times 10^{-19} \text{ cm}^2 \text{ eV}$. This value agrees with the calculated value within error limits. Resonances involving levels $4lnl'$ with $n \geq 7$ occur at energies above 5.6 keV, but modify our result only slightly because of the n^{-6} scaling; e.g., expanding the integration range to include the LNQ resonance increases the calculated value of S_{M2} only by about 10%.

In summary, we note that our results represent the first identification of the x-ray signature of indirect excitation processes in the x-ray spectrum of a highly charged ion interacting with a monoenergetic electron beam. Contributions from resonance excitation, recombination, and inner-shell ionization have been observed and their energy dependence has been determined.

We have found that $M2$ is strongly affected by indirect processes. Observations of neonlike iron from the Sun^{19,20} as well as neonlike germanium, selenium, and silver from the Princeton Large Torus²¹ found $M2$ to be substantially larger than predicted by models that included only direct electron-impact excitation and radiative cascades. Recent theoretical work has focused on contributions from resonance excitation to explain the discrepancy for iron.¹³ A study by Ruge and McKenzie²⁰ of the neonlike line emission of iron from solar flares showed that the relative line intensities calculated by Smith *et al.*¹³ with a model that included resonance contributions were too small to account for the observed intensities, especially at high electron temperatures. Subsequent calculations of the resonance contributions, including those based on the methods of Chen and Reed employed above, resulted in values which were even smaller than those of Smith *et al.*^{15,16} As our measurement of the resonance contribution is consistent with the more recent calculations, we conclude that indirect processes other than resonance excitation, i.e., recombination and ionization, which we have shown to be effective excitation mechanisms, are responsible for the large relative intensities of $M2$ in solar and tokamak observations and should not be neglected in model calculations for these plasmas.

We thank D. Nelson, E. Magee, and A. Hinz for expert technical support and M. Eckart and R. Fortner for their interest and encouragement. This work was performed under the auspices of the U.S. Department of

Energy at the Lawrence Livermore National Laboratory under Contract No. W-7405-Eng-48.

- ¹W. H. Goldstein *et al.*, Phys. Rev. Lett. **58**, 2300 (1987); B. K. F. Young *et al.*, Phys. Rev. Lett. **62**, 1266 (1989).
- ²M. Bitter *et al.*, Phys. Rev. A **32**, 3011 (1985); J. E. Rice, E. S. Marmor, E. Källne, and J. Källne, Phys. Rev. A **35**, 3033 (1987); E. Källne, in *Physics of Highly Ionized Atoms*, edited by R. Marrus (Plenum, New York, 1989).
- ³A. K. Pradhan, Astrophys. J. **288**, 824 (1985); R. Mewe, in Proceedings of the Conference on Atomic Spectra and Oscillator Strengths for Astrophysics and Fusion, Amsterdam, 1989, edited by J. Hansen [Phys. Scr. (to be published)]; D. A. Liedahl, S. M. Kahn, A. L. Osterheld, and W. H. Goldstein, Astrophys. J. **350**, L37 (1990).
- ⁴R. E. Marrs, M. A. Levine, D. A. Knapp, and J. R. Henderson, Phys. Rev. Lett. **60**, 1715 (1988).
- ⁵M. A. Levine, R. E. Marrs, J. R. Henderson, D. A. Knapp, and M. B. Schneider, Phys. Scr. **T22**, 157 (1988).
- ⁶E. D. Donets, Phys. Scr. **T3**, 11 (1983); R. Ali, C. P. Bhalala, C. L. Cocke, and M. Stockli, Phys. Rev. Lett. **64**, 633 (1990); R. W. Schmieder, in *Physics of Highly Ionized Atoms*, edited by R. Marrus, NATO Advanced Study Institutes, Ser. B, Vol. 201 (Plenum, New York, 1990), p. 321, and references therein.
- ⁷M. Loulergue and H. Nussbaumer, Astron. Astrophys. **24**, 209 (1973); J. H. Parkinson, *ibid.* **24**, 215 (1973).
- ⁸M. Klapisch *et al.*, Phys. Lett. **69A**, 34 (1978).
- ⁹M. Klapisch, Comput. Phys. Commun. **2**, 239 (1971); M. Klapisch, J. L. Schwob, B. S. Fraenkel, and J. Oreg, Opt. Soc. Am. **61**, 148 (1977).
- ¹⁰A. Bar-Shalom, M. Klapisch, and J. Oreg, Phys. Rev. A **38**, 1773 (1988).
- ¹¹J. R. Henderson *et al.*, Phys. Rev. Lett. **65**, 705 (1990).
- ¹²H. L. Zhang, D. H. Sampson, and R. E. H. Clark, Phys. Rev. A **41**, 198 (1990).
- ¹³B. W. Smith, J. C. Raymond, J. B. Mann, and R. D. Cowan, Astrophys. J. **298**, 898 (1985).
- ¹⁴G. Omar and Y. Hahn, Phys. Rev. A **37**, 1983 (1988).
- ¹⁵M. H. Chen and K. J. Reed, Phys. Rev. A **40**, 2292 (1989).
- ¹⁶W. H. Goldstein, A. Osterheld, J. Oreg, and A. Bar-Shalom, Astrophys. J. **344**, L37 (1989).
- ¹⁷The charge-exchange cross section was estimated from formulas given by A. Müller and E. Salzborn, Phys. Lett. **62A**, 391 (1977).
- ¹⁸B. M. Penetrante, M. A. Levine, and J. N. Bardsley, in *International Symposium on Electron Beam Ion Sources and their Applications*, edited by A. Hershcovitch, AIP Conference Proceedings No. 188 (American Institute of Physics, New York, 1989), p. 145; M. B. Schneider *et al.*, *ibid.*, p. 158.
- ¹⁹K. J. H. Phillips *et al.*, Astrophys. J. **256**, 774 (1982).
- ²⁰H. R. Rugge and D. L. McKenzie, Astrophys. J. **297**, 338 (1985).
- ²¹P. Beiersdorfer *et al.*, Phys. Rev. A **34**, 1297 (1986); P. Beiersdorfer, M. Bitter, S. von Goeler, and K. W. Hill, Nucl. Instrum. Methods Phys. Res., Sect. B **43**, 347 (1989).

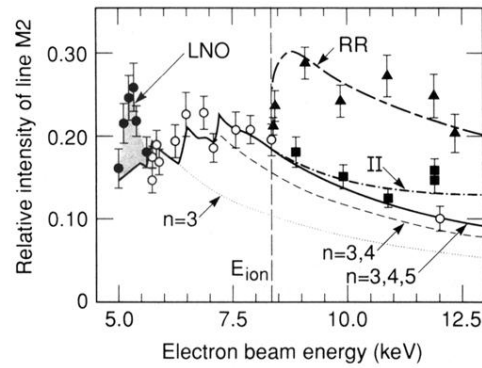


FIG. 1. Dependence of the relative intensity of line $M2$ on beam energy. The data are normalized to the intensity of line $3D$. Open circles reflect data excited predominantly by electron collisions and cascade feeding. Resonance excitation is strongest for data plotted as solid circles. Recombination of Ba^{47+} strongly affects data plotted as solid triangles; inner-shell ionization of Ba^{45+} affects the data plotted as solid squares. Also shown are the predictions from a collisional-radiative model which includes all $n=3$ levels (dotted line), all $n=3,4$ levels (dashed line), and all $n=3,4,5$ levels (solid line). The dot-dashed and long-short-dashed lines represent model calculations of the effects of inner-shell ionization (II) of Ba^{45+} and of radiative recombination (RR) of Ba^{47+} , respectively. In the latter calculation the radiative recombination coefficient has been increased by a factor of 5 to fit the data. E_{ion} denotes the ionization potential of Ba^{46+} at 8.33 keV.